PROCEEDINGS OF SCIENCE

Cosmology with galaxy redshift surveys at $z \sim 1$: results from the VIPERS

Luigi Guzzo[*†]
INAF - Osservatorio Astronomico di Brera, via E. Bianchi 46, 23807 Merate (LC), Italy
E-mail: luigi.guzzo@brera.inaf.it

Statistical measurements of large-scale structure in the local Universe are one of the pillars upon which the current "standard" model of cosmology rests. Such studies are now being pushed to higher redshifts by deeper surveys sampling significant volumes of the distant Universe. These allow us to sample the evolution of structure at different epochs, as well as the evolution of galaxies themselves within it. The VIMOS Public Extragalactic Redshift Survey (VIPERS) is one such survey, and the largest redshift survey ever conducted with the ESO telescopes. It has used the Very Large Telescope to target spectroscopically a sample of $100,000$ galaxies at $0.5 < z < 1.2$. With a combination of volume and sampling density that is unique for these redshifts, it allows statistical measurements of galaxy clustering and related cosmological quantities to be obtained on an equal footing with local results. At the same time, the simple magnitude-limited selection and the wealth of ancillary photometric data provide a general view of the galaxy population, its physical properties and the relation of the latter to large-scale structure. This paper presents an overview of the galaxy clustering results obtained so far with the VIPERS data, together with their cosmological implications. Most of these are based on the $\sim 55,000$ galaxies forming the first public data release (PDR-1). As of January 2015, observations and data reduction are complete and the final data set is being validated and made ready for the final investigations.

Frontiers of Fundamental Physics 14 - FFP14,
15-18 July 2014
Aix Marseille University (AMU) Saint-Charles Campus, Marseille

[*]Speaker.

[†]*On behalf of the VIPERS team* (http://vipers.inaf.it): U. Abbas, C. Adami, S. Arnouts, J. Bel, M. Bolzonella, D. Bottini, E. Branchini, A. Burden, A. Cappi, J. Coupon, O. Cucciati, I. Davidzon, S. de la Torre, G. De Lucia, C. Di Porto, P. Franzetti, A. Fritz, M. Fumana, B. Garilli, B. R. Granett, L. Guennou, A. Hawken, O. Ilbert, A. Iovino, J. Krywult, V. Le Brun, O. Le Fèvre, D. Maccagni, K. Malek, A. Marchetti, C. Marinoni, F. Marulli, H. J. McCracken, Y. Mellier, L. Moscardini, R. C. Nichol, L. Paioro, J. A. Peacock, W. J. Percival, S. Phleps, M. Polletta, A. Pollo, H. Schlagenhaufer, M. Scodeggio, A. Solarz, L. A. M. Tasca, R. Tojeiro, D. Vergani, M. Wolk, G. Zamorani, A. Zanichelli.

PoS(FFP14)016

1. Large-scale structure as a cosmological probe

Statistical measurements of large-scale structure in the galaxy distribution represent one of the pillars upon which the current "standard" model of cosmology rests. The power spectrum of this distribution contains a wealth of information on the history of cosmological fluctuations, which in principle allows precise constraints on cosmological parameters like the mean density of matter Ω_m and the baryon fraction. Additionally, galaxy clustering has emerged more recently as a powerful means to understand the origin of the apparent acceleration of cosmic expansion, discovered at the end of the last century [35, 32]. The tiny "baryonic wiggles" in the shape of the power spectrum are the mark of a specific spatial scale, the remnant of the sound horizon size at the baryon drag epoch. One of the major discoveries of the past decade has been that there are enough baryons in the cosmic mixture to influence the dominant dark-matter fluctuations [9, 18] and leave a visible signature in the galaxy distribution. Such Baryonic Acoustic Oscillations (BAO) represent a formidable standard ruler to measure the expansion history of the Universe $H(z)$, similar to what has been originally done using supernovae (see e.g. [1]). Additionally, the apparent anisotropy of clustering induced by the contribution of peculiar velocities to the measured redshifts, what we call Redshift Space Distortions (RSD, [26]), provides us with a precious complementary tool which probes the growth rate of structure. This key information can break the degeneracy in explaining the observed expansion history, between the presence of a cosmological constant in Einstein's equations or a rather more radical revision of these equations, which we call "modified gravity". While RSD are a well-known phenomenon since long, their potential in the context of understanding the origin of cosmic acceleration has been recognized only in recent times [21].

Translating galaxy clustering observations into precise and accurate cosmological measurements, however, requires careful modelling of the effects of non-linear evolution, galaxy bias (i.e. how galaxies trace mass) and redshift-space distortions themselves. Galaxy surveys collecting broad samples of the galaxy population with a simple, well-defined selection function and extensive photometric information are crucial to ease this. In general, they allow us to play with different classes of tracers of the underlying matter density field (e.g. red and blue galaxies, groups, clusters), which are differently affected by the above effects. This has been the case of the two largest surveys of the local Universe, i.e. the Sloan Digital Sky Survey (SDSS, [42]) and the 2dF Galaxy Redshift Survey (2dFGRS, [10]).

The VIMOS Public Extragalactic Redshift Survey (VIPERS) was conceived to extend this concept, with comparable statistical accuracy, to the $z \sim 1$ Universe, pursuing the following main goals:

- To precisely and accurately measure galaxy clustering up to scales $\sim 100\,h^{-1}$ Mpc at $z \sim 1$ and obtain cosmological constraints from the power spectrum and correlation function, at an epoch when the Universe was about half its current age.
- To measure the growth of structure through RSD out to $z \sim 1$, possibly using different populations of tracers, as allowed by the broad selection function.
- To characterize the density field at such redshifts, tracing the evolution and non-linearity of galaxy bias and identifying non-linear structures as groups and clusters.

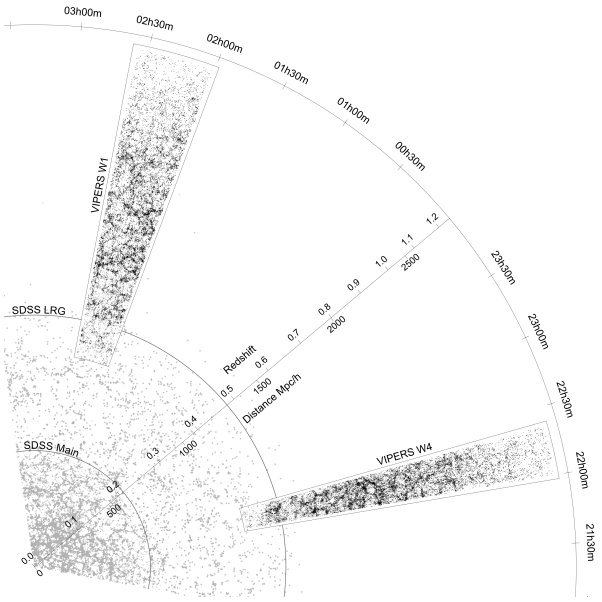

Figure 1: The large-scale distribution of galaxies within the two VIPERS survey volumes, integrated over the declination direction (1.84 and 1.54 degrees thick, respectively for W1 and W4). The new data are matched to the SDSS main and LRG samples at lower redshift (for which a 4-degree-thick slice is shown). Note how VIPERS pushes into a new epoch, with detailed sampling on all scales, similarly to SDSS Main below $z \sim 0.2$. Conversely, sparse samples like the SDSS LRG are excellent statistical probes of the largest scales, but (by design) fail to register the details of the underlying nonlinear structure.

- To precisely measure statistical properties of the galaxy population (luminosity, colour, stellar mass) and their relationship with large-scale structure.

To achieve this, VIPERS exploits the unique capabilities of the VIMOS multi-object spectrograph at the ESO VLT. This is used to measure redshifts for $\sim 10^5$ galaxies over ~ 24 square degrees and located at $0.5 < z < 1.2$. Galaxy targets are selected from the W1 and W4 fields of the Canada–France–Hawaii Telescope Legacy Survey Wide catalogue (CFHTLS–Wide), which provides high-quality photometry in five bands (*ugriz*).[1] The survey area is tiled with a mosaic of 288 VIMOS pointings. The target sample is magnitude-limited to $i_{AB} = 22.5$, and further constrained to $z > 0.5$ through a thoroughly-tested *ugri* colour pre-selection [22]. Discarding the $z < 0.5$ population allows us to nearly double the sampling density within the high-redshift volume of interest, reaching an average sampling $> 40\%$. At the same time, the area and depth correspond to a volume of 5×10^7 h^{-3} Mpc^3, comparable to that of the 2dFGRS at $z \sim 0$ [10]. Such a combination of sampling and volume is unique among redshift surveys at $z > 0.5$. VIPERS has used 372 hours of multi-object spectroscopy, plus 68.5 hours of pre-imaging, corresponding to an effective total investment of about 55 nights of VLT time. These and more details on the survey construction and the properties of the sample can be found in [22] and [20].

[1] http://terapix.iap.fr/rubrique.php?id_rubrique=252

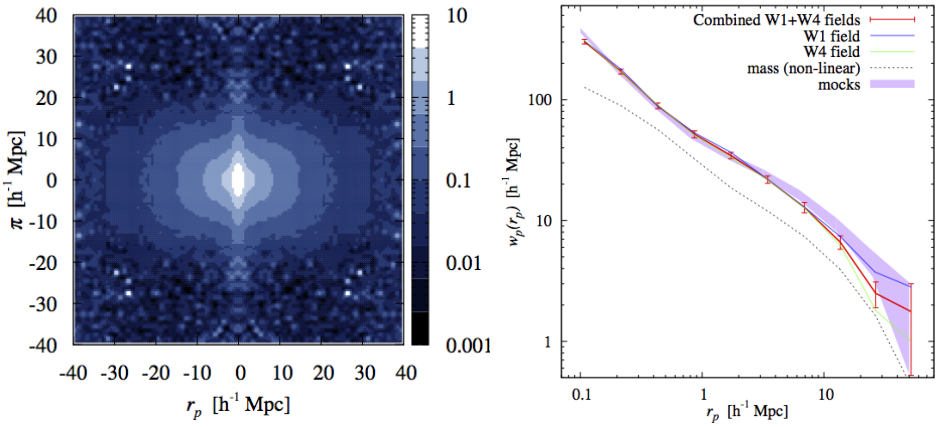

Figure 2: Redshift-space two-point correlation function over the full $0.5 < z < 1.0$ range, from the VIPERS PDR-1 catalogue. Left: $\xi(r_p, \pi)$, showing the well-defined signature of linear redshift distortions, i.e. the oval shape of the contours (de la Torre et al., 2013). Right: the projected correlation function $w_p(r_p)$, obtained by integrating $\xi(r_p, \pi)$ along the π direction, for W1 and W4 fields separately and for the total sample. These are compared to the best-fitting ÎŻ Cold Dark Matter model for the mass (dotted line, prediction using the HALOFIT code, [40]). The shaded area corresponds to the $1-\sigma$ error corridor, computed from the scatter in the measurements of a large set of mock surveys, custom built for VIPERS [**?**]delatorre13.

2. Galaxy clustering and cosmological parameters at $0.5 < z < 1.2$

The simplest, yet striking result of a redshift survey like VIPERS can be appreciated in the maps of the galaxy distribution shown in Fig. 1. The comparison of the two VIPERS wedges to the data of the local Universe evidences the remarkable combination of volume and dynamical range (in terms of scales sampled), which is a unique achievement of VIPERS at these redshifts. The two slices are about 2 degrees thick and display with great detail the cellular structure with which we have become familiar from local surveys and numerical simulations, but at an epoch when the Universe was about half its current age and for which no such detailed and extended map existed so far.

2.1 Redshift-space clustering and the growth of structure

One of the original goals of VIPERS is the measurement of the amplitude and anisotropy of the redshift-space two-point correlation function at redshift approaching unity. $\xi(r_p, \pi)$ and the corresponding projected function $w_p(r_p)$ from the first data release (PDR-1) catalogue are shown in the two panels of Fig. 2 [13].

The fingerprint of RSD is evident in the flattening of $\xi(r_p, \pi)$ along the line-of-sight direction (left panel of Fig. 2). The right panel shows the projected correlation function $w_p(r_p)$, obtained by projecting $\xi(r_p, \pi)$ along the line-of-sight direction. The agreement in shape and amplitude between W1 and W4 is remarkable.

Modelling $\xi(r_p, \pi)$, we have obtained a first estimate of the mean growth rate of structure at an effective redshift $z = 0.8$, $f\sigma_8 = 0.47 \pm 0.08$ [13]. Our measurement, conventionally expressed as

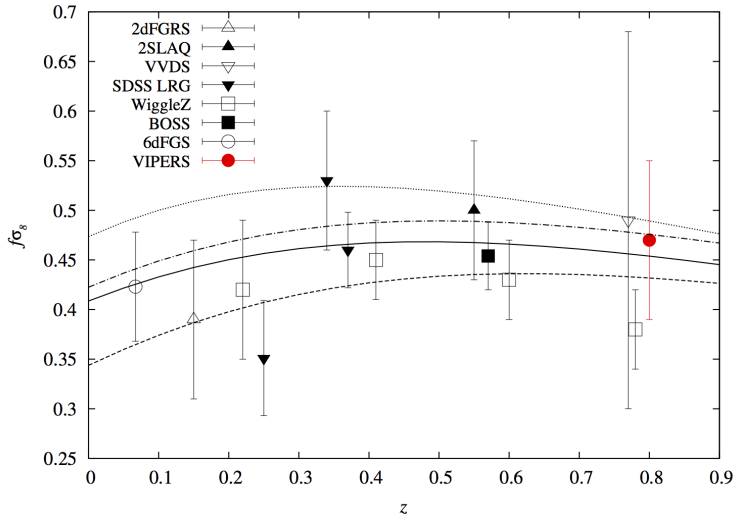

Figure 3: The growth rate of structure at $z \sim 0.8$ estimated from the VIPERS PDR-1 data [13]. This is expressed as the product $f\sigma_8$ and compared to a compilation of recent measurements, respectively from 2dFGRS [25], 2SLAQ [36], VVDS [21], SDSS LRG [6], WiggleZ [5], BOSS [34] and 6dFGS, [4]. Model predictions correspond to GR in a ΛCDM model with WMAP9 parameters (solid), while the dashed, dotted, and dot-dashed curves are respectively Dvali-Gabadaze-Porrati (dashed, [17], $f(R)$ (dotted), and coupled dark energy (dot-dashed) model expectations. For these latter two models, the analytical growth rate predictions from [14] have been used.

the product of the growth rate f with the *rms* amplitude of matter fluctuations, σ_8, is compared to a selection of literature results and models in Fig. 3, where the models have been self-consistently normalised to the Planck estimate of σ_8. The VIPERS value is in agreement with the predictions of general relativity within the current error bars. We expect the final VIPERS catalogue to push the error bars down to $\sim 10\%$, or to allow splitting the measurement into two bins with error comparable with the current one. We are also exploring the combined use of different tracers of RSD (e.g. blue and LRG galaxies, or groups [30]), as a way to reduce statistical and systematic errors, a specific advantage allowed by the high sampling and broad selection function of VIPERS.

2.2 The galaxy power spectrum at $z \sim 1$

The power spectrum in Fourier-space provides a complementary view to the correlation function of the spatial distribution of galaxies. Ideally, in Fourier space one could estimate the power spectrum in bins corresponding to independent wave modes k. In practice, the survey geometry and mask, especially in cases like VIPERS when the size in one direction is significantly smaller than the other two, give rise to a window function in Fourier-space which damps the power and couples modes. The specific window function must be accurately accounted for to compare models with the observations.

We present the VIPERS monopole power spectrum measurement in the left panel of Fig. 4 [37]. To account for the variation in galaxy bias over the extended redshift range of VIPERS, the sample is split into two redshift bins $0.6 \leq z \leq 0.9$ and $0.9 \leq z \leq 1.1$. To properly compare the

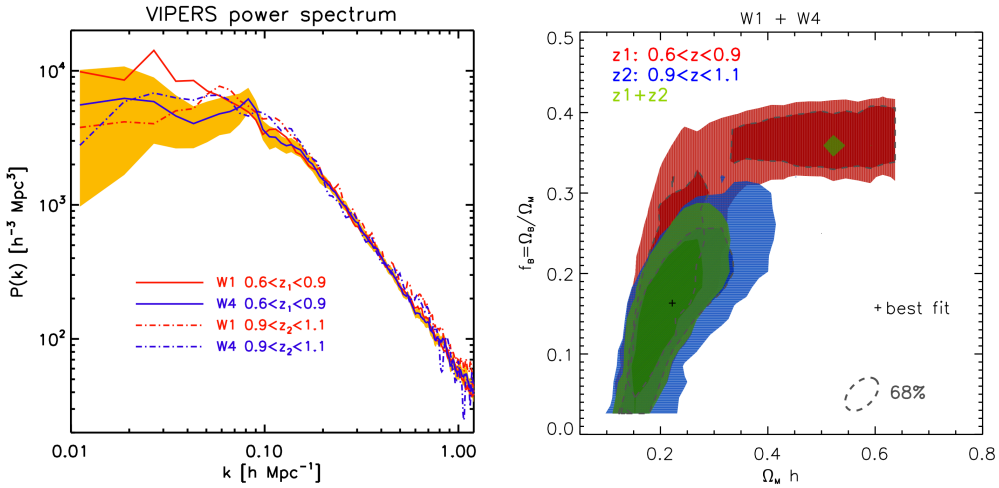

Figure 4: Left: Estimates of the three-dimensional power spectrum of the galaxy distribution from the VIPERS data. The four curves correspond to two redshift bins for the two separated fields W1 and W4, which have slightly different window functions. Right: corresponding constraints on the mean matter density and baryonic fraction. This plot can be directly compared to that at $z \sim 0.1$ from the 2df galaxy survey by [9]. See [37] for details.

measurements to theory, we must model the window functions separately for the two fields and the two redshift bins. We carry out a joint likelihood analysis of the four measurements containing the galaxy bias in each sample, the matter density and the baryon fraction. In the right panel of Fig. 4 we compare the constraints found from the full sample $0.6 \leq z \leq 1.1$ with those derived from the joint analysis of the two redshift sub samples. The degeneracy in the $\Omega_m - f_B$ plane is considerably lessened by splitting the sample into two redshift ranges. In [37] we explicitly show that the systematic dependence of the likelihood on the choice of the maximum wave number k_{max} to be included, is weaker for the high-redshift bin, where clustering is more linear. This bin is also providing a much tighter statistical constraint on the two considered quantities, driving the global likelihood contours. The right panel of Fig. 4 can be directly compared to Fig. 24 in [9], to notice how the constraining power of VIPERS, under the same assumptions, is similar to that of the 2dFGRS at low redshift. When we include the best available priors on H_0, n_s (from Planck) and $\Omega_b h^2$ (from BBN), we obtain a value $\Omega_{m,0} = 0.272^{+0.027}_{-0.030}$. This agrees within 1% with the independent analysis of the PDR-1 data using the *clustering ratio* $\eta_{g,R}$ (based on counts-in-cells, see [2] for details). Such an agreement between estimates in Fourier and configuration space is not at all obvious, given the way systematic effects can enter these computations.

The VIPERS targeting algorithm may be extended over the full ~ 130 square degree area of the CFHTLS photometric sample. Thus, by combining the three-dimensional clustering from VIPERS with a projected clustering measurements from CFHTLS, we may improve the constraining power of the two individual surveys. In this spirit, in a work that pre-dated the 2013 results from the PDR-1, we measured the projected power spectrum of the CFHTLS using the VIPERS target selection at $0.5 < z < 1.2$ [23] and used those measurements to constrain separately the total neutrino mass $\sum m_\nu$ and the effective number of neutrino species $N_{\rm eff}$ [43]. Combined with WMAP7 and adding

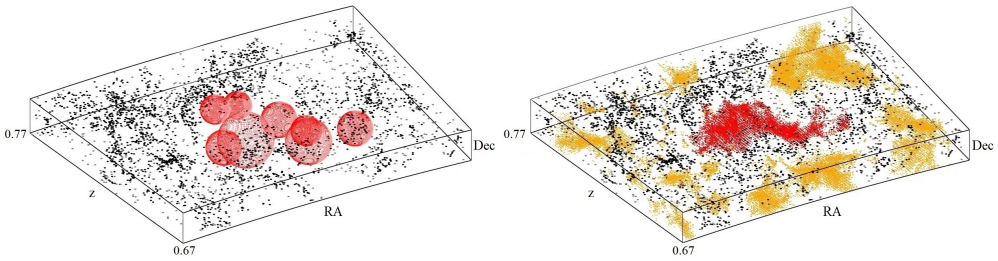

Figure 5: Identifying cosmic voids in the VIPERS PDR-1 W1 volume (see Micheletti et al. 2014 for details). This region includes the largest maximal sphere in the catalogue, which has a radius of 31 h^{-1} Mpc. The left-hand panel shows this sphere and the other six maximal spheres detected in this void region. The right-hand panel shows, in red, the centres of the overlapping significant spheres that make up the void, other void regions within this area of the survey are shown in orange. The grey and black points in both panels are the isolated and unisolated galaxies, respectively.

a prior on the Hubble constant yielded an upper limit of $\sum m_\nu < 0.29\,\mathrm{eV}$ and $N_{\rm eff} = 4.17^{+1.62}_{-1.26}$ (2σ confidence levels).

2.3 Galaxy bias and higher-order clustering

In [15], we used the PDR-1 data to study the biasing relation and its nonlinearity over the redshift range covered by VIPERS. This analysis is based on an improved version of the method originally proposed and developed in [12] and [39]. It entails estimating the 1-point PDF of galaxies from counts in cells of a given size and, assuming a model for the mass PDF, inferring the full bias relation. We detect small ($\lesssim 3$ %), but significant deviations from linear bias, with the mean biasing function being close to linear in regions above the mean density. The linear bias parameter increases both with luminosity and with redshift, with a strong bias evolution only for $z > 0.9$, in agreement with some, but not all, previous studies. Specifically, this indicates that the observed tension between the zCOSMOS and VVDS-Deep bias estimates at $z \sim 1$ is fully accounted for by cosmic variance. Such behaviour is confirmed by the recent mesurement of the three– and four–point correlation functions, together withe the normalised skewness and kurtosis of the galaxy density field [7].

2.4 Cosmic voids

VIPERS probes the galaxy density field to $z \sim 1$ with unprecedented fidelity, allowing us to experiment with additional tests of cosmological and galaxy formation models. Void statistics and profiles have gained popularity in recent times, thanks to the increased volumes sampled by redshift surveys [41]. The specific sampling of a redshift survey, i.e. its "resolution" in defining cosmic structures into the non-linear regime, however, is another important ingredient in order to properly define void catalogues. VIPERS, despite its nearly 2D "slice" geometry is one such survey, where the sampling density is nearly two orders of magnitude higher than surveys of much larger volume reaching similar redshifts (as e.g. the WiggleZ survey, [16]).

Voids have been identified in VIPERS over the range $0.55 < z < 0.9$, using search method based upon the identification of empty spheres that fit between galaxies, as shown in Fig. 5. This

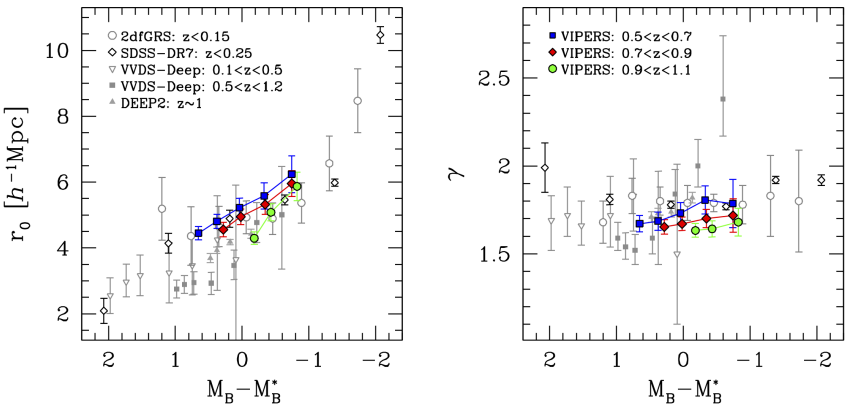

Figure 6: The dependence of clustering on galaxy luminosity (B-band absolute magnitude) as seen in VIPERS, compared to previous measurements at low and high redshift. The best-fit values of the correlation length r_0 and slope γ, for a power-law fit to the two-point correlation function, are plotted for three redshift slices of the PDR-1 catalogue.

allows us to characterise cosmic voids despite the presence of complex survey boundaries and internal gaps. The void size distribution and the void-galaxy correlation function are found to agree well with the equivalent functions in Λ-CDM mock catalogues [29]. The anisotropy of the void-galaxy cross correlation function indicates that galaxies are outflowing from voids. Modelling this can be used to put loose constraints on the growth rate of structure.

2.5 Dependence of clustering on galaxy luminosity and stellar mass

The dependence of galaxy clustering on the luminosity and stellar mass of the galaxy tracers is a well-established effect at low redshifts (e.g. [31]. At $z \sim 1$ results have been so far less conclusive, although both DEEP-2 [8] and VVDS-Deep [33] suggest a steepening of the two-point correlation function, when compared to local samples. This analysis has been repeated on the PDR-1 catalogue by [28] and the resulting dependence on luminosity is shown in Fig. 6. In the figure, the amplitude and slope derived from the projected function $w_p(r_p)$ are plotted and confronted with previous results. While the trend of r_0 seems to be consistent among surveys, both at low and high redshift, the strong steepening evidenced by VVDS-Deep at $z \sim 1$ (large value of γ, right panel), is not confirmed by the VIPERS data (green circles). In [28] we see similar trends when samples are selected based on ranges of stellar mass. In the same paper we provide a thorough discussion of the difficulties and biases that are intrinsic in studies of the clustering dependence on stellar mass, when using data that are flux-limited in origin.

2.6 Reconstruction of the galaxy density field

Properly accounting for the correlations between intrinsic galaxy properties and their spatial distribution can lead to improved estimates of the underlying matter clustering statistics and tighter constraints on cosmological parameters. To carry out a joint analysis, considering full covariances, we have recently turned to Bayesian methods [24, (Granett et al. 2015)]. We have modelled the

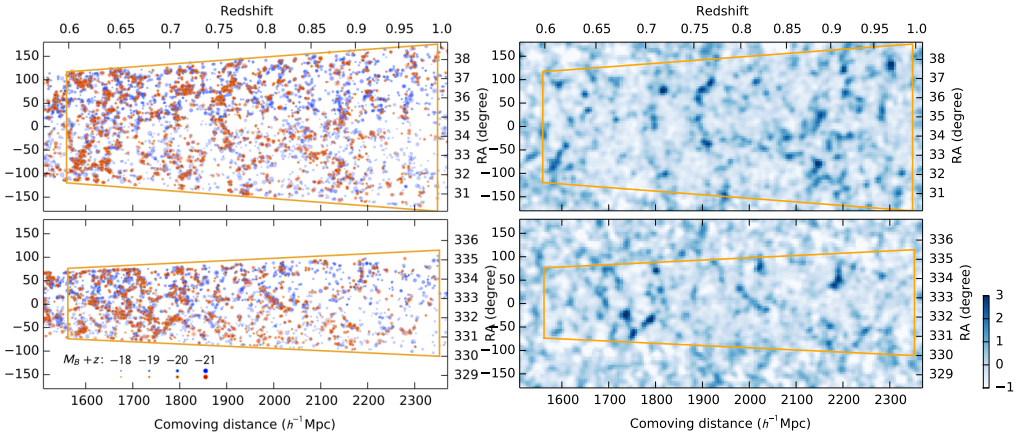

Figure 7: VIPERS cone diagrams for the fields W1 (top) and W4 (bottom). The left panels show the redshift-space positions of observed galaxies. The marker colour indicates the blue or red colour class and the marker size scales with B-band luminosity. The depth of the slice is $10h^{-1}$ Mpc . The orange line traces the field boundaries cut in the redshift direction at $0.6 < z < 1.0$. At right we show a slice of the density field taken from one step in the Markov chain. It represents the anisotropic Wiener reconstruction from the weighted combination of galaxy tracers. The field is filled with a constrained Gaussian realisation. The field has been smoothed with a Gaussian kernel with full-width-half-max $10h^{-1}$ Mpc . The colour scale gives the over-density value.

VIPERS galaxy counts as a function of luminosity and colour with a multivariate Gaussian distribution parameterised by the matter power spectrum, matter density, galaxy number density and galaxy bias. The high-dimensional parameter space is explored with Monte Carlo Gibbs sampling using the Wiener filter to reconstruct the density field. The Markov chain provides simultaneous reconstructions of the redshift-space density field and power spectrum as well as the galaxy biasing and luminosity functions. A slice through the galaxy distribution is shown in Fig. 7 alongside a Wiener density field reconstruction. The results of the Bayesian analysis, fully accounting for the covariances between galaxy properties and environment, give constraints on redshift-space clustering and galaxy intrinsic properties consistent with the individual VIPERS analyses, building a coherent picture of the cosmic density field [24].

3. Closing remarks

VIPERS is the first redshift survey reaching beyond $z = 1$ while providing simultaneously volume and sampling that are comparable to the best surveys of the local Universe. We are currently (January 2015) in the phase of validating the final $\sim 35,000$ redshifts. These will bring the final redshift sample close to 90,000 redshifts, out of $\sim 95,000$ targeted galaxies (plus 2500 contaminating stars). This completed sample will be used to produce definitive results on several of the large-scale structure investigations described here. In addition, it will enable specific new analyses, which have been waiting for the largest possible survey volume. These include, e.g., the construction of a group/cluster catalogue (Iovino et al., in preparation) or the combination of weak lensing

and RSD.

The parallel, very important results obtained with the VIPERS PDR-1 data in the field of galaxy evolution have not been discussed in this review, which focuses on large-scale structure. Among these, the precise measurement of the stellar mass function evolution over the $0.5 < z < 1.2$ range needs to be mentioned. This study benefits of the large volume sampled by VIPERS, to provide an unprecedented sampling of the massive end at $z \sim 1$ [11]. Also, a thorough study of the evolution of the Colour-Magnitude diagram and the galaxy luminosity function over the same range has been instead presented in [19].

Finally, VIPERS has distinguished itself for a very early public release of more than half of the survey data (the PDR-1 catalogue), in October 2013, i.e. only six months after submission of the first series of scientific papers. A similar policy will be followed for the complete survey data, for which we foresee a public distribution in 2016 (please monitor the survey web site, `http://vipers.inaf.it`, for related announcements). As a consequence, we expect (and encourage), a large number of further and important analyses, both on large-scale structure and galaxy evolution, to be produced by the scientific community at large.

References

[1] Anderson, L., et al. 2014, *MNRAS*, 441, 24

[2] Bel, J., & VIPERS Team 2014, *A&A*, 563, A37

[3] Bel, J. & Marinoni, C. 2014, *A&A*, 563, A36

[4] Beutler, F., et al. 2012, *MNRAS*, 423, 3430

[5] Blake, C., et al. 2011, *MNRAS*, 415, 2876

[6] Cabrè, A. & Gaztanñaga, E. 2009, *MNRAS*, 393, 1183

[7] Cappi, A., & VIPERS Team 2015, *A&A*, submitted

[8] Coil, A.L., et al. 2006, *ApJ*, 644, 671

[9] Cole, S., et al. 2005, *MNRAS*, 362, 505

[10] Colless, M., et al. 2001, *MNRAS*, 328, 1039

[11] Davidzon, I., & VIPERS Team 2013, *A&A*, 558, A23

[12] Dekel, A. & Lahav, O. 1999, *ApJ*, 520, 24

[13] de la Torre, S., Guzzo, L., Peacock, J. A., et al. 2013, *A&A*, 557, A54

[14] Di Porto, C., Amendola, L., & Branchini, E. 2012, *MNRAS*, 419, 985

[15] Di Porto, C., & VIPERS Team 2014, *A&A*, submitted (arXiv:1406.6692)

[16] Drinkwater, M.J., et al. 2010, *MNRAS*, 401, 1429

[17] Dvali, G., Gabadadze, G., & Porrati, M. 2000, Phys. Lett. B, 485, 208

[18] Eisenstein, D. J., et al. 2005, *ApJ*, 633, 560

[19] Fritz, A., & VIPERS Team 2014, 563, A92

[20] Garilli, B., & VIPERS Team 2014, 562, A23

[21] Guzzo, L., & VVDS Team 2008, *Nature*, 451, 541

[22] Guzzo, L., & VIPERS Team 2014, *A&A*, 566, A108

[23] Granett, B.R., & VIPERS Team 2012, *MNRAS*, 421, 251

[24] Granett, B.R., & VIPERS Team 2015, *A&A*, submitted

[25] Hawkins, E., et al. 2003, *MNRAS*, 346, 78

[26] Kaiser, N. 1987, *MNRAS*, 227, 1

[27] Kovač, K., et al. 2011, *ApJ*, 731, 102

[28] Marulli, F., & VIPERS Team 2013, *A&A*, 557, A17

[29] Micheletti, D., & VIPERS Team 2014, *A&A*, 570, A106

[30] Mohammad, F., et al. 2015, *MNRAS*, submitted (arXiv:1502.05045)

[31] Norberg, P., et al. 2001, *MNRAS*, 328, 64

[32] Perlmutter, S., et al. 1999, *ApJ*, 517, 565

[33] Pollo, A., & VIPERS Team 2006, *A&A*, 451, 409

[34] Reid, B. A., et al. 2012, *MNRAS*, 426, 2719

[35] Riess, A. G., et al. 1998, *AJ*, 116, 1009

[36] Ross, N. P., et al. 2007, *MNRAS*, 381, 573

[37] Rota, S., & VIPERS Team 2015, *A&A*, submitted

[38] Samushia, L., et al. 2013, *MNRAS*, 29, 1514

[39] Sigad, Y., Branchini, E., & Dekel, A. 2000, *ApJ*, 540, 62

[40] Smith, R. E., et al. 2003, *MNRAS*, 341, 1311

[41] Sutter, P. M., et al. 2012, *ApJ*, 761, 44

[42] York, D. G., et al. 2000, AJ, 120, 1579

[43] Xia, J.Q., et al. 2012, *JCAP*, 6, 10